Journal of Traditional and Complementary Medicine 10 (2020) 207–216

Contents lists available at ScienceDirect

Journal of Traditional and Complementary Medicine

journal homepage: http://www.elsevier.com/locate/jtcme

Differential effects of thymoquinone on lysophosphatidic acid-induced oncogenic pathways in ovarian cancer cells

Ji Hee Ha [a, b], Muralidharan Jayaraman [a, b], Rangasudhagar Radhakrishnan [a], Rohini Gomathinayagam [a, b], Mingda Yan [a], Yong Sang Song [c], Ciro Isidoro [d], Danny N. Dhanasekaran [a, b, *]

[a] Stephenson Cancer Center, The University of Oklahoma Health Sciences Center, Oklahoma City, OK, 73104, USA
[b] Department of Cell Biology, The University of Oklahoma Health Sciences Center, Oklahoma City, OK, 73104, USA
[c] Cancer Research Institute, Seoul National University, College of Medicine, Seoul, 151-921, South Korea
[d] Università del Piemonte Orientale, Novara, Italy

ARTICLE INFO

Article history:
Received 14 February 2020
Received in revised form
6 April 2020
Accepted 7 April 2020
Available online 12 April 2020

Keywords:
Ovarian cancer
LPA
Thymoquinone
Phytochemical
Anticancer

ABSTRACT

Thymoquinone, a therapeutic phytochemical derived from Nigella sativa, has been shown to have a potent anticancer activity. However, it has been identified that the tumor microenvironment (TME) can attenuate the anticancer effects of thymoquinone (TQ) in ovarian cancer. Lysophosphatidic acid (LPA), a lipid growth factor present in high concentration in the TME of ovarian cancer, has been shown to regulate multiple oncogenic pathways in ovarian cancer. Taking account of the crucial role of LPA in the genesis and progression of ovarian cancer, the present study is focused on assessing the efficacy of TQ in inhibiting LPA-stimulated oncogenic pathways in ovarian cancer cells. Our results indicate that TQ is unable to attenuate LPA-stimulated proliferation or metabolic reprogramming in ovarian cancer cells. However, TQ potently inhibits the basal as well as LPA-stimulated migratory responses of the ovarian cancer cells. Furthermore, TQ abrogates the invasive migration of ovarian cancer cells induced by Gαi2, through which LPA stimulates cell migration. TQ also attenuates the activation of JNK, Src, and FAK, the downstream signaling nodes of LPA-LPAR-Gαi2 signaling pathway. In addition to establishing the differential effects of TQ in ovarian cancer cells, our results unravel the antitherapeutic role of LPA in the ovarian cancer TME could override the inhibitory effects of TQ on cell proliferation and metabolic reprogramming of ovarian cancer cells. More importantly, the concomitant finding that TQ could still sustain its inhibitory effect on LPA-stimulated invasive cell migration, points to its potential use as a response-specific therapeutic agent in ovarian cancer.

1. Introduction

Thymoquinone (TQ) is a bioactive naturally occurring phytochemical derived from the seeds of the plant Nigella Sativa. Its chemopreventive and anti-tumorigenic effects are well-characterized.[1–4] TQ has been shown to have pleotropic anti-cancer effects including chemopotentiation, anti-inflammation, immunomodulation, and radiosensitization.[5] TQ has been shown to inhibit multiple tumorigenic signaling nodes such as those involved in cell proliferation, epithelial to mesenchymal transition, invasive cell migration, and metastasis in addition to inducing apoptosis in many different cancers.[1] In addition, TQ has been shown to enhance chemosensitivity in many cancers including cisplatin-response in ovarian cancer cell lines.[6–8] In ovarian cancer context, TQ has been demonstrated to induce both the inhibition of cell proliferation and induction of apoptosis.[9–11] However, using mouse model of ovarian cancer, it has also been noted that the tumor microenvironment can limit the efficacy of the anti-oncogenic effects of TQ.[11] Our previous *in vivo* and in vitro studies have shown that the lipid growth factor LPA, synthesized and secreted by the ovarian cancer cells is present in high concentration in the ascites of ovarian cancer patients.[12–14] With

* Corresponding author. Stephenson Cancer Center, The University of Oklahoma Health Sciences Center, Oklahoma City, OK, 73104, USA.
E-mail address: danny-dhanasekaran@ouhsc.edu (D.N. Dhanasekaran).
Peer review under responsibility of The Center for Food and Biomolecules, National Taiwan University.

https://doi.org/10.1016/j.jtcme.2020.04.001

List of abbreviations

GAPDH	Glyceraldehyde 3-phosphate dehydrogenase
LPA	Lysophosphatidic Acid
LPAR	Lysophosphatidic Acid Receptor
TQ	Thymoquinone
FAK	Focal Adhesion Kinase
ROS	Reactive Oxygen Species
JNK	Jun n-terminal kinase

its ability to stimulate multiple oncogenic signaling pathways in ovarian cancer cells as well as cancer-associated fibroblasts, LPA has been identified as the critical growth factor present in the ovarian cancer TME. While the pleotropic effects of thymoquinone (TQ) are extensively studied, no studies thus far have investigated the anti-cancer effects of TQ in the presence of LPA in ovarian cancer. Therefore, in the present study, we investigated whether LPA has any negative effect on the anticancer inhibitor activities of TQ on LPA-induced proliferation, migration, and metabolic programming in ovarian cancer cells. Results from our study indicated that while TQ does not affect the LPA-stimulated proliferation or metabolic reprogramming of ovarian cancer cells. Rather, TQ stimulated these responses in a context-dependent manner. On the contrary, TQ potently inhibited both basal and LPA-induced cell migration and invasion of a panel of ovarian cancer cells. Analyses of the downstream signaling pathways indicated that the inhibition of cell migration and invasion by TQ could be corelated with the attenuation of LPA-stimulated motogenic signaling nodes comprising Jun kinase JNK), Src and Focal Adhesion Kinase (FAK). Collectively, our results point to two therapeutically relevant correlates: 1) TQ has no inhibitory effect on basal or LPA-induced cell proliferation and metabolic reprogramming in ovarian cancer cells; and 2) Nonetheless, TQ is able to inhibit LPA-induced invasive cell migration and associated oncogenic signaling nodes, thus identifying its potential as a response-specific therapeutic phytochemical *in vivo*. Furthermore, these findings provide an experimental paradigm in which the differential effects of TQ in the presence and absence of LPA could be analyzed so that improved strategies for effective cancer prevention and therapy could be developed.

2. Materials and Methods

2.1. Cell lines

OVCA429, SKOV3, HeyA8, OVCAR3, and OVCAR8 cells were cultured and maintained as previously described.[12,15,16] Patient derived cell line ASC022415 was isolated from the ascites samples of patients at the Stephenson Cancer Center, University of Oklahoma Health Science Center, Oklahoma City, OK, USA as described previously.[12] The study was approved by the OUHSC Office of Human Research Participant Protection Institutional Review Board and samples were collected with the consent of the patients. The ascites derived ovarian cancer cells were maintained in MCDB: DMEM (1:1) supplemented with 10% FBS and 50 μg/mL streptomycin. For serum-starvation, the above media without serum was supplemented with 0.1% BSA Fraction V, heat-shock, fatty acid ultra-free (Roche, Indianapolis, IN), 50 U/mL penicillin and 50 μg/mL streptomycin (Mediatech). Lysophosphatidic acid (1-oleoyl-2-hydroxy-sn-glycero-3-phosphate) was obtained from Avanti Polar Lipids (Alabaster, AL) and dissolved into 10 mM stock solutions in PBS with 0.1% BSA and stored at −80 °C until use. Thymoquinone (2-Isopropyl-5-methylbenzo-1,4-quinone), obtained from Cayman Chemical (Ann Arbor, MI), was dissolved into 10 mM stock solution in DMSO and stored in −20 °C until use. The concentrations of thymoquinone and LP that were determined by dose response curves for each cell-types and the optimal concentration at the linear range of the curve was used in these studies. All cells were transfected with a Nucleofector II system from Lonza (Allendale, NJ) using the provided transfection protocol for cells following our previously published methods. 2×10^6 cells per transfection cuvette were transfected with Gαi2QL (5 μg) or pcDNA3 (5 μg vector) as indicated. After transfection, the cells were plated on 60 mm plates and allowed to adhere overnight. The following day the media were changed and the cells were allowed to grow for 48 h. Transfectants were serum-starved for 18 h and treated with TQ, LPA, or TQ + LPA along with vehicle controls.

2.2. Cell proliferation assay

5-bromo-2′-deoxyuridine (BrdU) assay. BrdU incorporation was carried out according to previously published procedures with some modifications.[17] HeyA8 and OVCA429 cells were grown on 12-mm cover slips in 6-well plates. Following serum starvation for 16 h, these cells were treated with DMSO or Thymoquinone (TQ) (10 μM) for 1 h and stimulated with LPA (10 μM) or none for 24 h. At 22 h, the cells were pulsed with 1x solution (1 μM) of 5-bromo-2-deoxyuridine (Calbiochem, EMD Chemicals Inc.) for 2 h. Cells were fixed by 3% paraformaldehyde, and the DNA was denatured using 2 M HCl. The fixed cells were washed 3 times with PBS and incubated with 1:200 dilution of monoclonal BrdU antibodies (EMD Chemicals Inc.) for 1 h followed by 1:200 dilution of goat anti mouse IgG labeled with Alexa Fluor 488 dye (#A-11001; Thermo Fisher). Cells were co-stained with DAPI (0.5 μg/mL; Roche Molecular Biochemicals) for nuclear staining to monitor the total number of cells. Slides were mounted with ProLong Gold antifade reagent (Invitrogen). BrdU-labeled as well as DAPI-stained total cells were analyzed using a Nikon Eclipse TE2000 inverted epi-fluorescence microscope (20x magnification). Using ImageJ software (National Institutes of Health), the number of BrdU-labeled cells in relation to DAPI-labeled total number of cells was calculated. Results were expressed as a percentage of S phase cells (mean ± SEM, n = 3).

2.3. Cell migration assays

Automated single cell tracking migration assay: OVCAR8 cells, cultured in RPMI1640 medium were seeded in serum-free medium at a density of 10,000 cells per well into collagen-coated CellCarrier-96 Ultra microplate (6055708, PerkinElmer). After overnight cultivation, cell migration was stimulated by addition of 10% FBS. Live cell imaging was performed using an Operetta high-content imaging system equipped with a temperature and CO_2 control option set to 37 °C and 5% CO_2 (PerkinElmer). Directly after addition of the compounds, microplates were placed onto the pre-heated Operetta system and incubated for 30 min. After incubation, digital phase contrast images were acquired at 10X magnification (10X high NA objective) using Operetta's automatic digital phase contrast algorithm. Digital phase contrast images were acquired using a 20X high NA objective for 24 h at imaging intervals of 15 min. Migrating cells were tracked and imaged using automated single cell tracking algorithm of the Harmony high-content imaging and analysis software (PerkinElmer).

Ex vivo wound healing assay: Ex vivo wound healing assay was carried out as described previously by our group.[16,18] 5×10^5 cells were seeded into 60 mm culture dishes in 10% FBS media and allowed to adhere overnight. Cells were then washed three times with PBS and incubated in serum-deprived media for 24 h. A linear

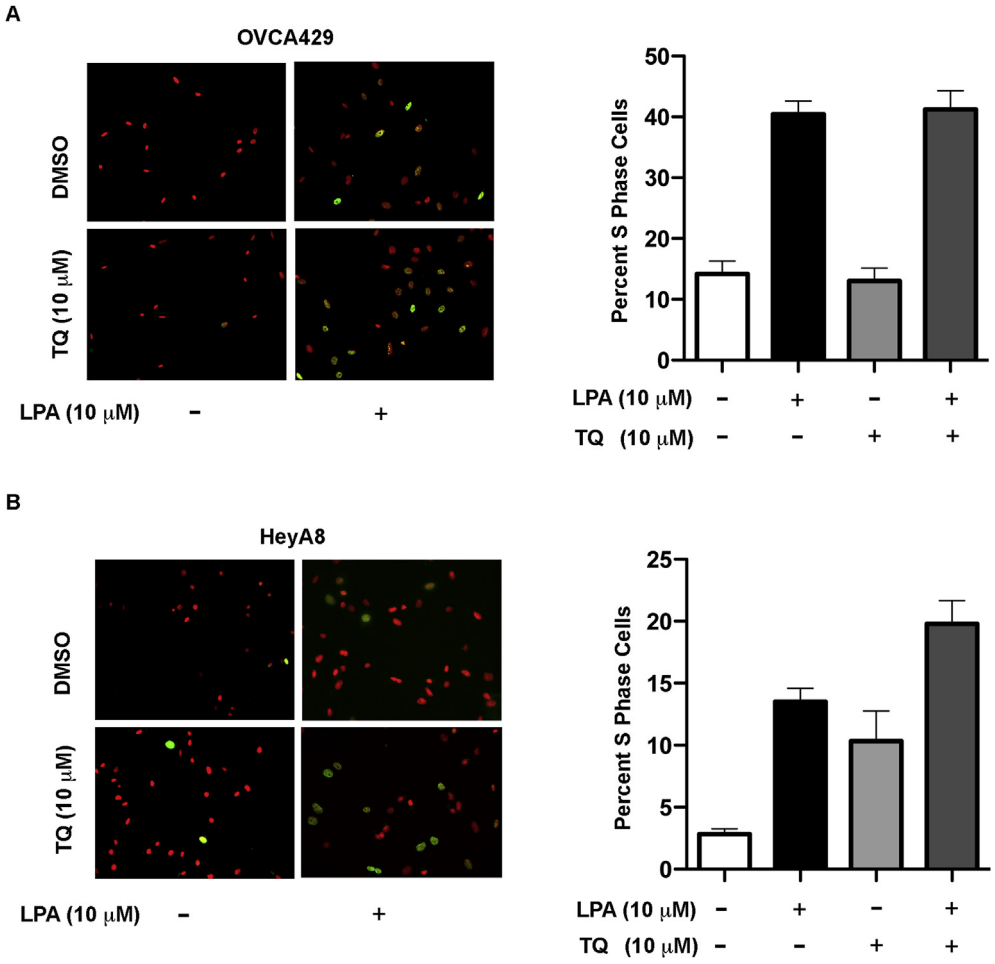

Fig. 1. Effect of TQ on LPA-stimulated Proliferation of Ovarian Cancer Cells. HeyA8 and OVCA429 cells were grown on coverslips. The cells were serum starved then treated with TQ (10 μM) and stimulated with LPA (10 μM). BrdU was pulsed and stained as described in the Methods. Stained OVCA429 (*A*) and HeyA8 (*B*) cells were imaged using Nikon Eclipse TE2000 inverted epifluorescent microscope (20x magnification). Percent S phase cells were quantified as ratio of BrdU (green) to DAPI (red) stained cells (Mean ± SEM; n = 3). Results are presented as percent S phase cells (*Right Panels*).

scratch wound was made across the cell monolayer using the sharp end of a 200 μL sterile pipette tip. The cells were washed with serum-free media to remove cellular debris. Fields of view (at 100× magnification) were selected at random along the linear wounds and imaged using an Olympus CK40 microscope and Kodak DC290 camera system. The photographed fields were marked with a felt tip marker to allow re-identification at the next time-point. The cells were then incubated with serum-free media containing 10 μM LPA, or serum-free media alone for the control. After 24 h incubation, the fields of view were identified and re-imaged.

Invasive Cell Migration Assay: Cell migration was monitored using a transwell chamber assay as previously described.[12,16,18,19] Cell culture inserts (polyethylene terephthalate membrane with 8.0 μm pores #353097, BD Biosciences, Franklin Lakes, NJ) were coated with rat-tail collagen, type 1 (BD Biosciences). 5×10^4 cells in 200 μL serum-free media were placed in the well of the companion plate. The companion plate wells contained 500 μL of control serum-free media and serum-free media with 10 μM LPA or 10% FBS. The cells were incubated for 20 h and the non-migrating cells on the proximal side of the inserts were removed with a cotton swab. The migrated cells on the distal side of the insert were fixed and stained with Hema color (EMD Chemicals, Inc., Gibbstown, NJ). Migrated cells were then enumerated with the images obtained from random fields of view at 10X magnification.

2.4. Seahorse XFe96 Extracellular Flux analysis

The extracellular acidification rate (ECAR) was determined in Seahorse XFe96 Extracellular Flux analyzer (Agilent, Billerica, MA) using the XF Glycolysis Stress Kit, according to the manufacturer's instructions, following our previously published methods.[12,13] Initial analyses were carried out with cell numbers ranging from 1×10^4 cells/well to 6×10^4 cells/well with 1×10^4 cells increment and observed that there were no cell number dependent changes in the experimental results. Results using 2×10^4 cells/well are presented. The data was analyzed and exported using the Seahorse Wave software (Agilent, Billerica, MA) to the GraphPad Prism (La Jolla, CA) to obtain the graphs and bar charts and also carry out statistical analyses.

2.5. Immunoblot analysis

Antibodies to Gαi2 (Sc-7276), ERK (sc-154), and FAK (sc-557) were from (Santa Cruz Biotechnology, Dallas, TX) whereas antibodies to JNK (9258), Src, Phospho-ERK1/2 (4370), p-JNK (9251), Src (2123), p-Src-Tyr416 (2101), p-FAK (3281), GAPDH (5174) were from Cell Signaling (Beverly, MA). Amersham ECL HRP-conjugated anti-rabbit IgG (NA9340V) and anti-mouse IgG (NA931V) were purchased from GE Healthcare Life Sciences (Madison, WI).

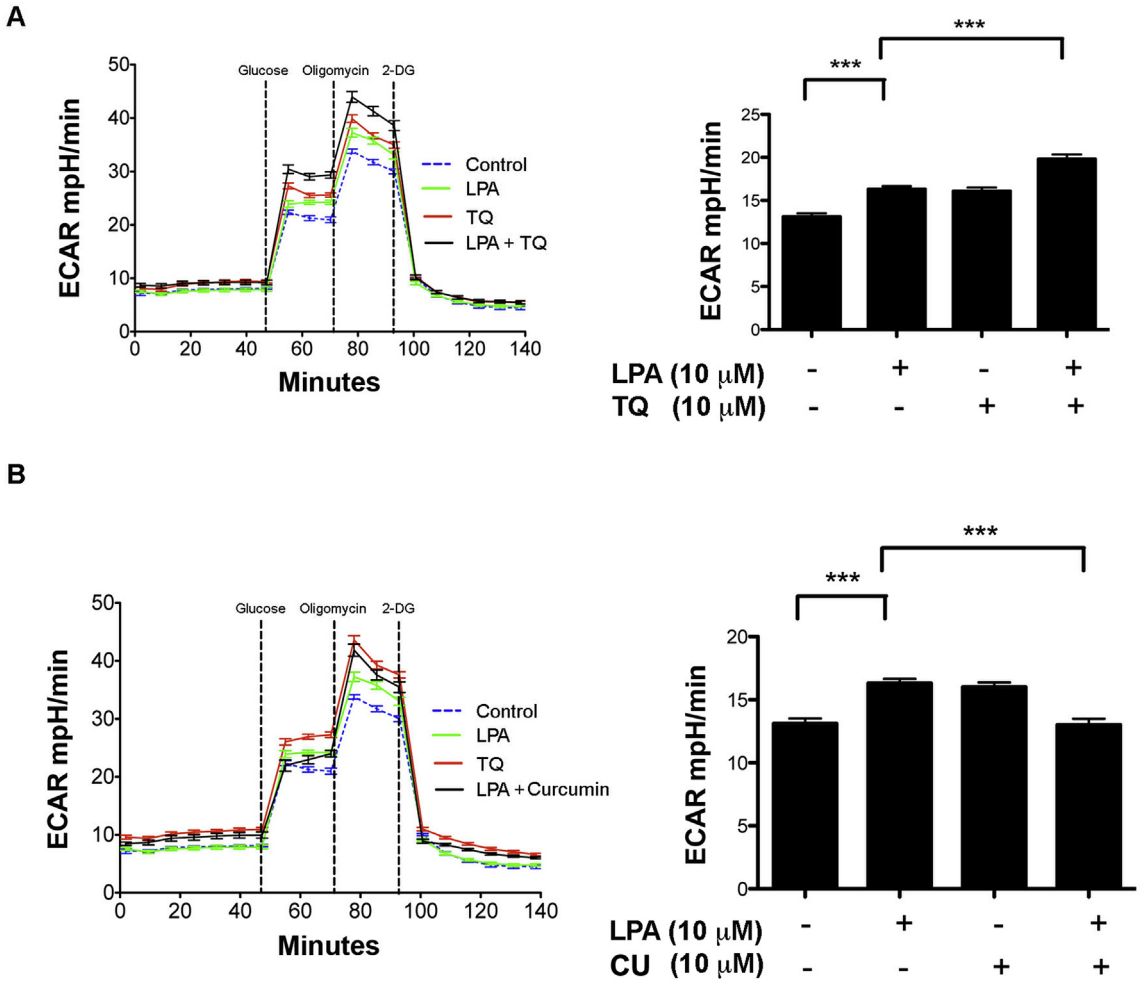

Fig. 2. Effect of TQ on LPA-induced metabolomic reprogramming of ovarian cancer cells. ASC022415 cells derived from ovarian cancer patient were pretreated with 10 μM TQ (*A*) or 10 μM Curcumin (*B*) for 1 h, following which, they were stimulated with LPA (10 μM) for 6 h. ECAR flux (*Left Panel*) and glycolytic rate (*Right Panel*) were plotted. Representative analysis from a set of three independent experiments (mean ± SEM; n = 9) is presented. Statistical significance was determined by Student *t*-test (***, P < 0.0005).

Immunoblot analyses were carried out according to our previously published methods.[18–20] The blots were developed using Super-Signal West Dura Extended Duration Substrate Reagent (34076) from Thermo Fisher Scientific (Waltham, MA). The blots were imaged using Kodak Image Station 4000 MM.

Statistical analysis: All statistical analysis was performed using GraphPad Prism (La Jolla, CA) by two-tailed student's *t*-test with Welch's correction.

3. Results

3.1. Effect of TQ on LPA-stimulated proliferation of ovarian cancer cells

Antiproliferative effect of TQ is well characterized to inhibit the proliferation of diverse types cancer cells.[21] We have shown previously that LPA, a lipid growth factor present in the ascites of ovarian cancer TME, stimulates the proliferation of ovarian cancer cells through the activation of its cognate G-protein couple receptors and downstream G proteins. In light of the observation that TME limits the efficacy of TQ in ovarian cancer, we investigated whether LPA could impede the inhibitory effect of TQ on the proliferation of ovarian cancer cells. This was carried out using OVCA429 cells that were treated with TQ in the presence or absence of 10 μM LPA along with the appropriate non-treated controls. Cell proliferation was monitored using nucleotide incorporation assay using BrdU. Our results indicated that LPA stimulated cell proliferation by in OVCA429 cells (Fig. 1A) and HeyA8 (Fig. 1B) cells. However, pretreatment of these cells with 10 μM TQ failed to have any inhibitory effect on LPA-induced proliferation in these cells, suggesting that TQ does not affect the basal or LPA-induced proliferation in ovarian cancer cells. Our results with HeyA8 cell line, which is derived from murine xenograft, indicated that TQ-treatment stimulated the proliferation in HeyA8 cells even in the absence of LPA.

3.2. Effect of TQ on LPA-induced metabolomic reprogramming of ovarian cancer cells

Many cancer cells resort to aerobic glycolysis to meet the increased biosynthetic and energy needs of the tumor growth and progression.[22,23] One of the anticancer effects of TQ relates to its ability to inhibit aerobic glycolysis in cancer cells.[24] We have recently demonstrated that LPA induces glycolytic shift in ovarian cancer cells to augment the biosynthetic and energy needs of the cancer cells. Therefore, we tested whether TQ could inhibit aerobic glycolysis induced by LPA using ovarian cancer patient-derived cells. Results from our analysis indicated that LPA stimulated

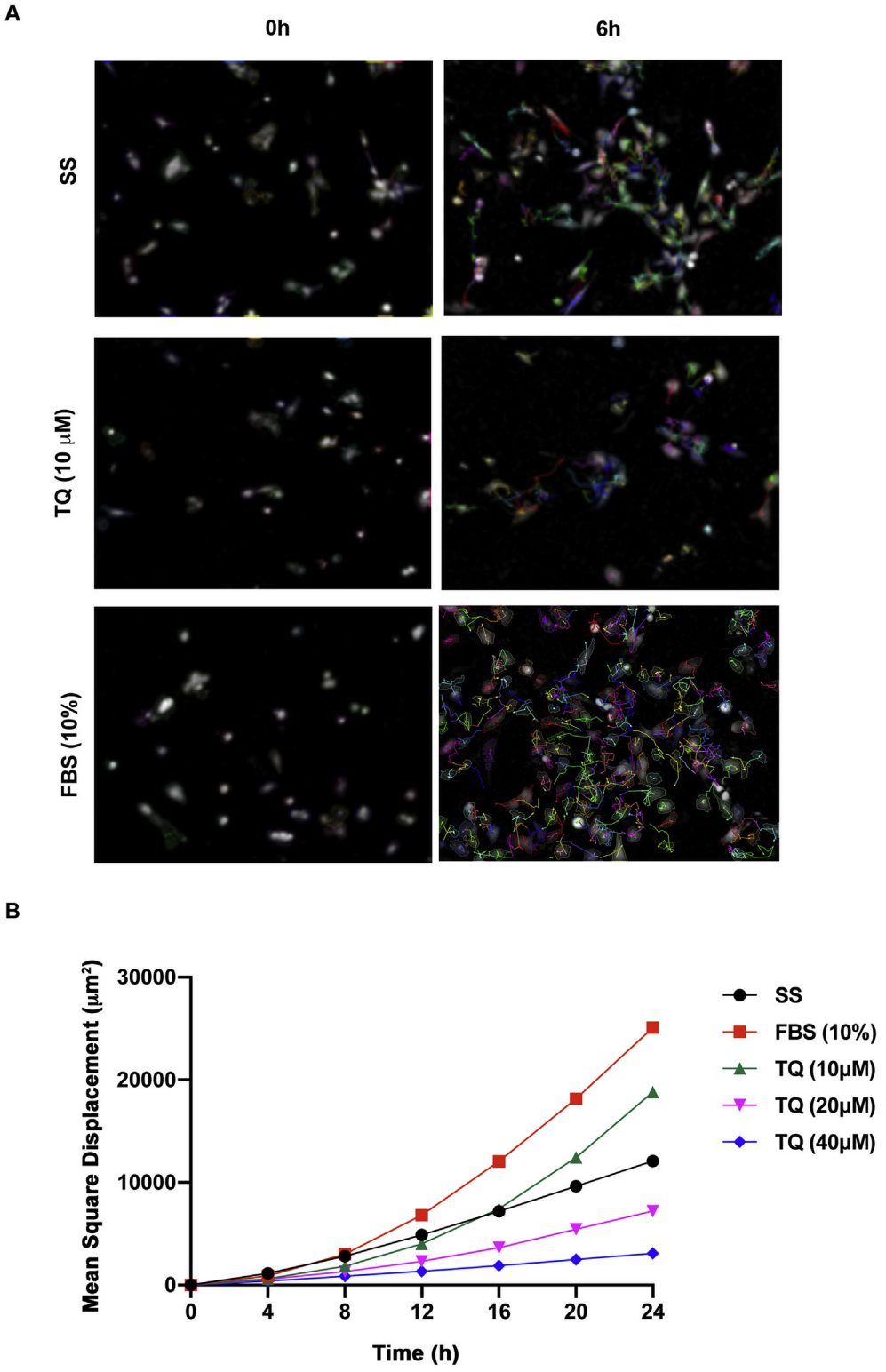

Fig. 3. Effect of TQ on ovarian cancer cell migration. OVCAR8 cells (10^4) were plated in 96-well plate in serum free media. After 16 h of incubation, the cells were treated with FBS (10%) or TQ (10, 20, or 40 μM). Every 15 min digital phase contrast images were captured on PerkinElmer Operetta for 24 h. Cell displacement was tracked using Harmony 4.3 software and representative cell tracked images (*A*) are presented. Mean square displacement, accumulated over time for all of the cells were quantified and presented (*B*).

glycolytic shift in these ASC022415 cells as previously reported by us.[12] However, TQ failed to inhibit such LPA-induced glycolytic shift in these cells (Fig. 2A). In contrast, curcumin, which was used as a positive control in these cells, abrogated the stimulatory response elicited by LPA (Fig. 2B).

3.3. Effect of TQ on LPA-induced cell migration and invasion

LPA has been well characterized to promote migration and invasion of ovarian cancer cells.[25] Therefore, we investigated whether the ability to inhibit ovarian cancer cell migration and invasion

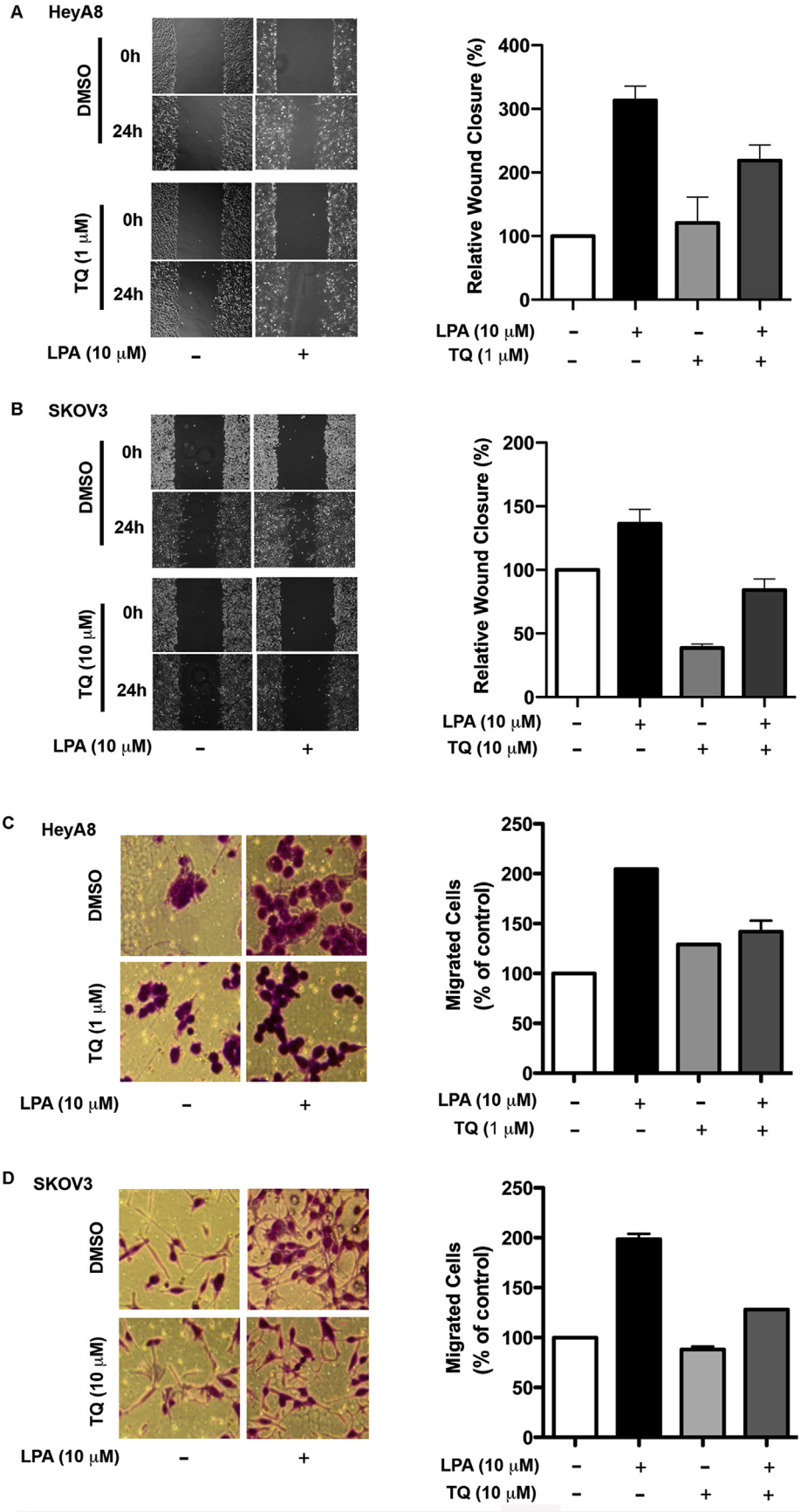
A
HeyA8
DMSO
0h
24h
TQ (1 μM)
0h
24h
LPA (10 μM) – +
Relative Wound Closure (%)
400
300
200
100
0
LPA (10 μM) – + – +
TQ (1 μM) – – + +
B
SKOV3
DMSO
0h
24h
TQ (10 μM)
0h
24h
LPA (10 μM) – +
Relative Wound Closure (%)
200
150
100
50
0
LPA (10 μM) – + – +
TQ (10 μM) – – + +
C
HeyA8
DMSO
TQ (1 μM)
LPA (10 μM) – +
Migrated Cells (% of control)
250
200
150
100
50
0
LPA (10 μM) – + – +
TQ (1 μM) – – + +
D
SKOV3
DMSO
TQ (10 μM)
LPA (10 μM) – +
Migrated Cells (% of control)
250
200
150
100
50
0
LPA (10 μM) – + – +
TQ (10 μM) – – + +

could be compromised by LPA. We carried out initial analysis to confirm the potential of TQ to inhibit motogenic response in ovarian cancer cells. This was carried out by live cell imaging using an automated single cell tracking migration assay in Operetta Hight Content Imaging system. OVCAR8 cells were serum-starved and cell migration was monitored in the presence of 10% FBS with or without the pretreatment of different concentration of TQ. Control cells showed weaker cell migration as indicated by the shorter cell tracks exhibited by a fewer number of cells (Fig. 3A). In the presence of serum, the motogenic response is greatly increased with a greater number of cells showing longer cell tracks. More importantly, the pretreatment of the cells with TQ inhibited the migration of these cells. A temporal analysis with different doses of TQ further confirmed the ability of TQ to inhibit and decelerate the rate of migration of ovarian cancer cells as indicated by the dose-dependent decrease in the mean square displacement rate over time (Fig. 3B).

Next, we analyzed the ability of TQ to inhibit LPA-stimulated cell migration of ovarian cancer cells using an *ex vivo* wound-healing assay. SKOV3 or HeyA8 cells, pretreated with TQ, were stimulated with 10 μM LPA along with appropriate controls. Our results indicated that TQ drastically inhibited LPA-stimulated migration of these cells (Fig. 4A and B). To interrogate the effect of TQ on LPA-stimulated invasive migration of these cells, we monitored the migration of these cells treated as above using collagen I-coated transwell assay. As shown in Fig. 4C and D, TQ potently inhibited LPA-stimulated invasive migration in both the ovarian cancer cell lines.

3.4. TQ attenuates LPA-induced motogenic signaling nodes

Focusing on defining the motogenic signaling nodes targeted by TQ in LPA-stimulated cells, we investigated the effect of TQ on the putative downstream signaling nodes regulated by LPA-LPAR signaling. Our recent studies have shown a critical role for LPA-stimulated Gαi2 in ovarian cancer cell migration.[26–28] Constitutively activated mutants of Gαi2 has been shown to activate the downstream signaling responses in a receptor-independent manner.[26–28] Therefore, we interrogated whether the activated mutant of Gαi2 could stimulate invasive migration of ovarian cancer cells and if so, whether TQ could inhibit such response. As shown in Fig. 5A, the expression of the activated mutants of Gαi2 stimulated the invasive migration of OVCAR3 cells by more than 50% (66%) in these cells.

Next, we investigated the effect of TQ on the signaling pathways activated by LPA-LPAR-Gαi2 in promoting invasive cell migration. We have previously shown that LPA-LPAR-Gai2-signaling nexus stimulates invasive migration of ovarian cancer cells through the activation of JNK, Src, and FAK.[15,27,28] Therefore, we investigated whether TQ inhibits LPA-stimulated activation of any or all of these kinases. SKOV3-ip cells that were stimulated with LPA, following which they were treated with 10 μM TQ for 1 h. Cells were lysed and the lysates were subjected to immunoblot analyses using antibodies to the Jun kinase, Src, or FAK. The blots were stripped and reprobed with the antibodies for the respective activated kinases. As shown in Fig. 5B, TQ robustly inhibited the activation of JNK,[15,29] c-Src, and FAK, all of which have been identified by us and others as regulatory signaling nodes involved in LPA-mediated migration and invasion of ovarian cancer cells.[26,27,30] Together, our results indicate that while LPA could override the inhibitory effect of TQ on cell proliferation and metabolic programming, TQ proves effective in inhibiting the motogenic nodes regulated by serum as well as LPA in ovarian cancer cells.

4. Discussion

The medicinal use of Nigella sativa - from which TQ has been extracted - dates back to at least two millennia.[31] Anticancer activity of TQ as well as its chemopreventive role has been well established in many cancer models characterized.[1–4] However, using a xenograft mouse model of ovarian cancer, it has been observed that the long-term treatment of TQ has a deleterious effect in ovarian cancer xenograft growth with the attenuation of its therapeutic efficacy.[11] The observed blunting of the therapeutic activity of TQ was attributed to “microenvironmental effects”. LPA forms the major autocrine and paracrine oncogenic lipid growth factor in TME of ovarian cancer. We demonstrate here that the effects of TQ are attenuated by LPA in a context-specific manner and we identify LPA as one of the tumor-microenvironmental factors that can alter the efficacy of TQ. While TQ had little or no effect on cell proliferation (Fig. 1) or metabolic reprogramming (Fig. 2A), it potently inhibited the invasive cell migration or motogenic response stimulated by LPA (Figs. 3–5). While TQ had no effect on the basal or LPA-stimulated proliferation of OVCA429 cells (Fig. 1A), it stimulated the basal proliferation rate of HeyA8 cells (Fig. 1B). It is significant to note here that HeyA8 cells were originally obtained from an ovarian cancer cell line derived xenograft that was passaged through immune-deficient mouse.[32,33] Many of the xenograft-derived human cancer cell lines often lose their original characteristics due to adaptive changes they have undergone in response to the murine tumor microenvironment.[34] Thus, it is possible that the atypical response observed in HeyA8 cells is due to the altered phenotype of HeyA8 cells, primed by the murine TME. It is of interest to note here that the observed pro-mitogenic effect of TQ is somewhat analogous to the TME-induced pro-tumorigenic effect of TQ observed in ovarian cancer xenografts in mouse.[11] Further analyses with a greater number of xenograft-derived cells should be able to define the mechanism underlying pro-mitogenic effects of TQ in cells. In addition, we have shown previously that ovarian cancer cells synthesize and release LPA in the culture medium, forming an autocrine stimulatory loop.[13] Thus, it is possible that the failure of TQ to inhibit cell proliferation in OVCA429 cells (Fig. 1A) could also be due to the presence of such autocrine loop. Considering the fact that ovarian cancer is continuously bathed in ascites that contain high concentration of LPA, it can be envisaged that LPA in the tumor microenvironment of ovarian cancer modulates the activities of TQ.

Fig. 4. Effect of TQ on LPA-induced migration and Invasion of ovarian cancer cells. Effect of TQ on cell migration was determined using an *ex vivo* wound-healing assay. HeyA8 (*A*) or SKOV3 cells (*B*) were plated (1×10^6 cells/dish) and allowed to adhere overnight. Cell were serum-starved for 16 h and treated with 0.5 μM Mitomycin-C to arrest cell division. Linear scratch wounds were made with 200 μL pipette tips across the monolayer of cells to initiate the wound-healing assay. Cells were pretreated with TQ for 1 h and stimulated with 10 μM LPA along with appropriate controls. At 0 h, fields of view (10x) were selected at random, photographed and marked for re-identification. The identical fields were re-imaged after 24 h of incubation. The images presented are representative of three independent experiments, each performed with triplicate fields of view. Percentage of wound closure and the migration inhibition percentage were quantified. Error bars are presented as mean ± SEM for triplicate experiments (*Right Panels*). The effect of TQ on invasive cell migration was carried out using a transwell assay. HeyA8 (*C*) or SKOV3 (*D*) cells suspended in 200 μL (5×10^4), serum-free media were placed in the upper well of the transwell insert. Each well of the companion plate contained 500 μL media containing serum-free media (control) or serum-free media containing 10 μM LPA (LPA) with or without TQ (10 μM). The cells were incubated for 24 h. Nonmigrating cells on the proximal side of the inserts were removed with a cotton swab and the migrated cells on the distal side of the insert were fixed stained with Hemacolor. Images were obtained of random fields of view at 10X magnification. The images shown are representative of the 3 independent experiments, each performed with triplicate fields. Migrated cells were quantified from three independent experiments (mean ± SEM; n = 3) and plotted as percent migrated cells over control (*Right Panel*).

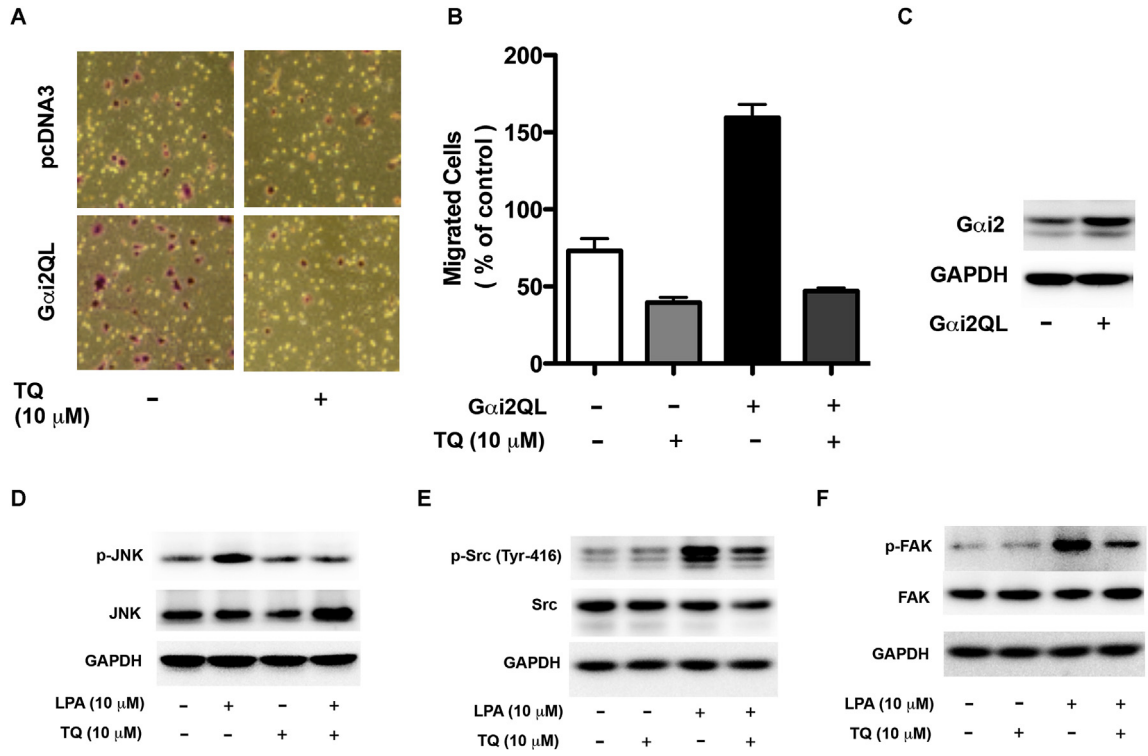

Fig. 5. Effect of TQ on LPA-stimulated motogenic signaling nodes. Inhibitory effect of TQ on the invasive migration stimulated by the activated mutant of Gαi2 was carried out using the transwell assay as described under Materials and Methods. Invasive migratory response of OVCAR8 cells transiently expressing the constitutively activated mutant of Gαi2 (Gαi2QL) along with pcDNA3 vector control cells were subjected to transwell assay with or without TQ (10 μM). At 24 h, images were obtained from random fields of view at 10X magnification. Presented images are representative of three independent experiments, each carried out with triplicate fields of view (*A*). Cell migration profiles were quantified by recording the number of migrated cells in three different fields from three independent experiments (Mean ± SEM; n = 3). Results were plotted as percent migrated cells over control (*B*). Expression of the transfected Gαi2QL was monitored by immunoblot analysis using antibodies to Gαi2. The blot was stripped and reprobed with GAPDH to monitor equal loading of protein (*C*). Effect of TQ on the activation profile JNK, Src, and FAK were monitored using the SKOV3 cells. Serum starved SKOV3 cells were pretreated with TQ (10 μM) for 1 h then stimulated with LPA (10 μM) for 10 min. Lysates from these cells were analyzed for the activation of JNK (*D*), Src (*E*) and FAK (*F*) by immunoblot analysis for phosphorylation of the proteins. The blot was stripped and re-probed with antibodies to GAPDH to monitor equal loading of proteins. Results from a representative experiment are presented (n = 3).

It should also be noted here that TQ treatment led to an increase in the basal as well as LPA-stimulated glycolytic activity in these cells (Fig. 2A). Although the mechanism by which TQ increases the glycolytic shift in ovarian cancer cells was not interrogated in the present study, this can be attributed primarily to the ability of TQ to induce the generation of ROS.[24,35] Our previous studies have shown that LPA-induced glycolytic shift in ovarian cancer cells involve the generation of ROS.[12] Thus, it is more likely that the ROS generated by TQ promotes glycolytic shift synergizing with LPA in this process. Curcumin was used only as a positive control in this study to demonstrate its ability to inhibit LPA-induced glycolytic shift (Fig. 2B). In this regard, it is of significance to note that curcumin effectively inhibits LPA-induced glycolytic shift as opposed to TQ (Fig. 2B). This finding has significant chemopreventive and therapeutic value as it indicates that the anticancer effect(s) of TQ could be compensated by other phytochemicals that are insensitive to LPA.

While TQ was not effective in inhibiting LPA-stimulated cell proliferation and metabolic reprogramming, it potently inhibited LPA-stimulated invasive cell migration, which is critical for intraperitoneal metastatic spread of the disease. We have previously shown that LPA stimulated the migration of ovarian cancer cells through the stimulation of G-protein coupled LPA-receptors (LPARs).[15,26–28] We have also shown that LPA-LPAR stimulated cell migration involves the activation of downstream Src and FAK kinases through the stimulation of G protein Gi2.[15,26–28] Our studies demonstrating the ability of TQ to inhibit invasive cell migration stimulated by the activated mutant of Gαi2 and the downstream JNK, Src, and FAK, indicate that the signaling nodes targeted by TQ are downstream of the G-protein Gi2 (Fig. 5). While the present study does not focus on defining the mechanisms by which TQ inhibits these kinases, previous studies have shown that TQ could inhibit the activation of JNK in a context specific manner through the inhibition of the upstream kinase Apoptosis signal-regulating kinase 1 or interleukin-1 receptor-associated kinase 1.[36,37] Similarly, TQ has also been shown to inhibit the activation of Src through the induction of Src homology-2 phosphatase with the resultant inhibition of Src- and downstream FAK-activities.[38–40]

As summarized in Fig. 6, TQ exhibits a complex multiplexed mode of activities in ovarian cancer cells. Its inhibitory or stimulatory effect on cell proliferation appears to be cell-type dependent with no effect LPA-stimulated proliferative response. In the case of metabolic reprogramming of ovarian cancer cells, TQ rather stimulates and synergizes with LPA in promoting metabolic reprogramming. However, TQ retains its anticancer activity in ovarian cancer cells by potently inhibiting the basal as well as LPA-stimulated invasive migration of ovarian cancer cells. Based on this paradigm, it can be concluded that the anticancer activity of TQ on LPA-regulated oncogenic responses in ovarian cancer cells appears to be cellular context- and response-specific. It is more likely that similar context- and response-specific tumor microenvironmental cues are involved in mitigating the anticancer efficacy of other phytochemicals in other cancers as

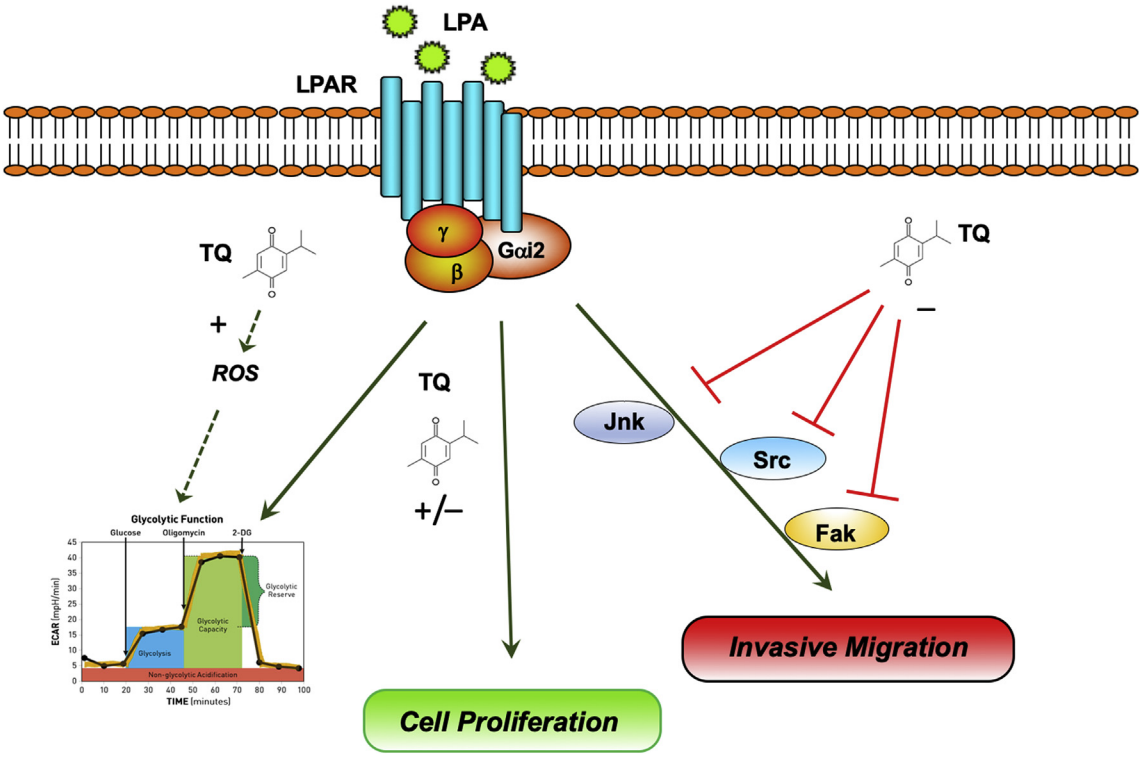

Fig. 6. Schematic Representation of the differential effects of TQ on LPA-stimulated oncogenic pathways in ovarian cancer cells. TQ stimulates and synergizes (+) with the metabolic reprogramming induced by LPA via its receptor (LPAR) in ovarian cancer cells. The dotted line represents the potential role of ROS in mediating this effect. TQ had no effect (OVCA429) or stimulatory effect (HeyA8) on ovarian cancer cells in a context-specific manner (+/−). TQ potently inhibits (−) both the basal and LPA-induced invasive migration by down regulating the activities of JNK, Src, and FAK that are downstream of LPA-LPAR-Gαi2 signaling in a panel of ovarian cancer cells.

well. From a clinical point of view, defining the response-specific anticancer activities of phytochemicals in the presence of the cancer-specific tumor microenvironmental factors could lead to the development of effective combination therapy with complementary phytochemicals for cancer prevention and adjuvant therapy.

Declaration of competing interest

The authors declare that there is no conflict of interest.

Acknowledgement

This research was supported by National Institutes of Health grant GM103639 and Stephenson Cancer Center, OUHSC, Oklahoma City, OK (to D.N. Dhanasekaran). Research reported in this publication was supported in part by the National Cancer Institute Cancer Center Support Grant P30CA225520 and Institutional Development Award (IDeA) from the National Institute of General Medical Sciences of the National Institutes of Health grant P20 GM103639 awarded to the University of Oklahoma Health Sciences Center and used the Biospecimen and Tissue Pathology Shared Resource and Cancer Functional Genomics of the Molecular Biology and Cytometry Research Shared Resource. The content is solely the responsibility of the authors and does not necessarily represent the official views of the National Institutes of Health.

Appendix A. Supplementary data

Supplementary data to this article can be found online at https://doi.org/10.1016/j.jtcme.2020.04.001.

References

1. Asaduzzaman Khan M, Tania M, Fu S, Fu J. Thymoquinone, as an anticancer molecule: from basic research to clinical investigation. *Oncotarget*. 2017;8(31):51907–51919.
2. Mahmoud YK, Abdelrazek HMA. Cancer: thymoquinone antioxidant/pro-oxidant effect as potential anticancer remedy. *Biomed Pharmacother*. 2019;115:108783.
3. Goyal SN, Prajapati CP, Gore PR, et al. Therapeutic potential and pharmaceutical development of thymoquinone: a multitargeted molecule of natural origin. *Front Pharmacol*. 2017;8:656.
4. Khan MA, Tania M, Fu J. Epigenetic role of thymoquinone: impact on cellular mechanism and cancer therapeutics. *Drug Discov Today*. 2019;24(12):2315–2322.
5. Mostofa AGM, Hossain MK, Basak D, Bin Sayeed MS. Thymoquinone as a potential adjuvant therapy for cancer treatment: evidence from preclinical studies. *Front Pharmacol*. 2017;8:295.
6. Nessa MU, Beale P, Chan C, Yu JQ, Huq F. Synergism from combinations of cisplatin and oxaliplatin with quercetin and thymoquinone in human ovarian tumour models. *Anticancer Res*. 2011;31(11):3789–3797.
7. Wilson AJ, Saskowski J, Barham W, Yull F, Khabele D. Thymoquinone enhances cisplatin-response through direct tumor effects in a syngeneic mouse model of ovarian cancer. *J Ovarian Res*. 2015;8:46.
8. Huq F, Yu JQ, Beale P, et al. Combinations of platinums and selected phytochemicals as a means of overcoming resistance in ovarian cancer. *Anticancer Res*. 2014;34(1):541–545.
9. Shoieb AM, Elgayyar M, Dudrick PS, Bell JL, Tithof PK. In vitro inhibition of growth and induction of apoptosis in cancer cell lines by thymoquinone. *Int J Oncol*. 2003;22(1):107–113.
10. Liu X, Dong J, Cai W, Pan Y, Li R, Li B. The effect of thymoquinone on apoptosis of SK-OV-3 ovarian cancer cell by regulation of bcl-2 and bax. *Int J Gynecol Canc*. 2017;27(8):1596–1601.
11. Wilson AJ, Saskowski J, Barham W, Khabele D, Yull F. Microenvironmental effects limit efficacy of thymoquinone treatment in a mouse model of ovarian cancer. *Mol Canc*. 2015;14:192.
12. Ha JH, Radhakrishnan R, Jayaraman M, et al. LPA induces metabolic reprogramming in ovarian cancer via a pseudohypoxic response. *Canc Res*. 2018;78(8):1923–1934.
13. Radhakrishnan R, Ha JH, Jayaraman M, et al. Ovarian cancer cell-derived lysophosphatidic acid induces glycolytic shift and cancer-associated fibroblast-phenotype in normal and peritumoral fibroblasts. *Canc Lett*. 2019;442:

464–474.
14. Xu Y. Lysophospholipid signaling in the epithelial ovarian cancer tumor microenvironment. *Cancers*. 2018;10(7).
15. Ha JH, Yan M, Gomathinayagam R, et al. Aberrant expression of JNK-associated leucine-zipper protein, JLP, promotes accelerated growth of ovarian cancer. *Oncotarget*. 2016;7(45):72845–72859.
16. Gomathinayagam R, Muralidharan J, Ha JH, Varadarajalu L, Dhanasekaran DN. Hax-1 is required for Rac1-Cortactin interaction and ovarian carcinoma cell migration. *Genes Cancer*. 2014;5(3-4):84–99.
17. Lanier TL, Berger EK, Eacho PI. Comparison of 5-bromo-2-deoxyuridine and [3H]thymidine for studies of hepatocellular proliferation in rodents. *Carcinogenesis*. 1989;10(7):1341–1343.
18. Goldsmith ZG, Ha JH, Jayaraman M, Dhanasekaran DN. Lysophosphatidic acid stimulates the proliferation of ovarian cancer cells via the gep proto-oncogene galpha(12). *Genes Cancer*. 2011;2(5):563–575.
19. Radhika V, Onesime D, Ha JH, Dhanasekaran N. Galpha13 stimulates cell migration through cortactin-interacting protein Hax-1. *J Biol Chem*. 2004;279(47):49406–49413.
20. Kumar RN, Ha JH, Radhakrishnan R, Dhanasekaran DN. Transactivation of platelet-derived growth factor receptor alpha by the GTPase-deficient activated mutant of Galpha12. *Mol Cell Biol*. 2006;26(1):50–62.
21. Banerjee S, Padhye S, Azmi A, et al. Review on molecular and therapeutic potential of thymoquinone in cancer. *Nutr Canc*. 2010;62(7):938–946.
22. Fernandez-de-Cossio-Diaz J, Vazquez A. Limits of aerobic metabolism in cancer cells. *Sci Rep*. 2017;7(1):13488.
23. Lunt SY, Vander Heiden MG. Aerobic glycolysis: meeting the metabolic requirements of cell proliferation. *Annu Rev Cell Dev Biol*. 2011;27:441–464.
24. Park JE, Kim DH, Ha E, et al. Thymoquinone induces apoptosis of human epidermoid carcinoma A431cells through ROS-mediated suppression of STAT3. *Chem Biol Interact*. 2019;312:108799.
25. Kundu J, Chun KS, Aruoma OI, Kundu JK. Mechanistic perspectives on cancer chemoprevention/chemotherapeutic effects of thymoquinone. *Mutat Res*. 2014;768:22–34.
26. Ward JD, Dhanasekaran DN. LPA stimulates the phosphorylation of p130Cas via Galphai2 in ovarian cancer cells. *Genes Cancer*. 2012;3(9-10):578–591.
27. Ward JD, Ha JH, Jayaraman M, Dhanasekaran DN. LPA-mediated migration of ovarian cancer cells involves translocalization of Galphai2 to invadopodia and association with Src and beta-pix. *Canc Lett*. 2015;356(2 Pt B):382–391.
28. Ha JH, Ward JD, Radhakrishnan R, Jayaraman M, Song YS, Dhanasekaran DN. Lysophosphatidic acid stimulates epithelial to mesenchymal transition marker Slug/Snail2 in ovarian cancer cells via Galphai2, Src, and HIF1alpha signaling nexus. *Oncotarget*. 2016;7(25):37664–37679.
29. Imran M, Rauf A, Khan IA, et al. Thymoquinone: a novel strategy to combat cancer: a review. *Biomed Pharmacother*. 2018;106:390–402.
30. Bian D, Su S, Mahanivong C, et al. Lysophosphatidic acid stimulates ovarian cancer cell migration via a ras-MEK kinase 1 pathway. *Canc Res*. 2004;64(12):4209–4217.
31. Trang NT, Wanner MJ, Phuong le VN, Koomen GJ, Dung NX. Thymoquinone from eupatorium ayapana. *Planta Med*. 1993;59(1):99.
32. Selby PJ, Thomas JM, Monaghan P, Sloane J, Peckham MJ. Human tumour xenografts established and serially transplanted in mice immunologically deprived by thymectomy, cytosine arabinoside and whole-body irradiation. *Br J Canc*. 1980;41(1):52–61.
33. Buick RN, Pullano R, Trent JM. Comparative properties of five human ovarian adenocarcinoma cell lines. *Canc Res*. 1985;45(8):3668–3676.
34. Yada E, Wada S, Yoshida S, Sasada T. Use of patient-derived xenograft mouse models in cancer research and treatment. *Future Sci OA*. 2018;4(3). FSO271.
35. Woo CC, Kumar AP, Sethi G, Tan KH. Thymoquinone: potential cure for inflammatory disorders and cancer. *Biochem Pharmacol*. 2012;83(4):443–451.
36. Umar S, Hedaya O, Singh AK, Ahmed S. Thymoquinone inhibits TNF-alpha-induced inflammation and cell adhesion in rheumatoid arthritis synovial fibroblasts by ASK1 regulation. *Toxicol Appl Pharmacol*. 2015;287(3):299–305.
37. Hossen MJ, Yang WS, Kim D, Aravinthan A, Kim JH, Cho JY. Thymoquinone: an IRAK1 inhibitor with in vivo and in vitro anti-inflammatory activities. *Sci Rep*. 2017;7:42995.
38. Li F, Rajendran P, Sethi G. Thymoquinone inhibits proliferation, induces apoptosis and chemosensitizes human multiple myeloma cells through suppression of signal transducer and activator of transcription 3 activation pathway. *Br J Pharmacol*. 2010;161(3):541–554.
39. Kolli-Bouhafs K, Boukhari A, Abusnina A, et al. Thymoquinone reduces migration and invasion of human glioblastoma cells associated with FAK, MMP-2 and MMP-9 down-regulation. *Invest N Drugs*. 2012;30(6):2121–2131.
40. Westhoff MA, Serrels B, Fincham VJ, Frame MC, Carragher NO. SRC-mediated phosphorylation of focal adhesion kinase couples actin and adhesion dynamics to survival signaling. *Mol Cell Biol*. 2004;24(18):8113–8133.